Turbo-FSK, a Physical Layer for Low Power Wide Area Networks: Analysis and Optimization

Yoann Roth, Jean-Baptiste Doré, Laurent Ros, Vincent Berg

Turbo-FSK, a Physical Layer for Low Power Wide Area Networks: Analysis and Optimization

Yoann Roth[a,b,*], Jean-Baptiste Doré[a], Laurent Ros[b], Vincent Berg[a]

[a] *CEA, LETI, MINATEC Campus, F-38054 Grenoble, France*
[b] *Univ. Grenoble Alpes, GIPSA-Lab, F-38000 Grenoble, France*

Abstract

As the Internet-of-Things is becoming a reality, the need for a new Low Power Wide Area (LPWA) network emerged in the last few years. Numerous low cost devices will be connected and this requires an optimization of the link budget: the physical layer needs to be designed highly energy efficient. The combination of M-ary orthogonal Frequency-Shift-Keying (M-FSK) modulation and coding in the same process has been shown to be a promising candidate when associated to an iterative receiver (turbo principle). In this work, we study this new digital transmission scheme, called Turbo-FSK. An EXtrinsic Information Transfer (EXIT) Chart analysis is realized. The influence of the packet length is investigated, and the scheme is shown to stay energy efficiency even with short packet sizes. Comparison with LPWA current technologies is performed, showing the potential of this technology.

Keywords: Turbo FSK, Low rate, Internet of Things (IoT), Low Power Wide Area (LPWA)

Résumé

L'Internet des Objets devient une réalité, et depuis plusieurs années le besoin d'un nouveau réseau longue portée basse consommation est apparu. Le but de ce réseau est de connecter un grand nombre de nœuds à faible coût, tout en optimisant le bilan de liaison. La couche physique doit alors être définie très efficace énergétiquement. La combinaison de la modulation orthogonale de fréquence à M états avec un codage canal dans un processus conjoint, et non successif, à l'émission se révèle très efficace lorsqu'un récepteur itératif est utilisé. Ce papier concerne l'étude de cette technique Turbo-FSK avec l'outil d'analyse itérative EXIT (EXtrinsic Information Transfer, en anglais). La métrique est adaptée au cas de la M-FSK et l'influence de la taille du paquet est étudiée. On montre alors que la technique reste performante même lorsque que la taille de paquet est réduite. La comparaison avec des techniques actuelles est réalisée, montrant le potentiel de la technologie proposée.

1. Introduction

Energy is a major concern when it comes to embedded systems; some systems will harvest the surrounding sources of energy, other will use low power components to save it. In the context of wireless communication systems, the technique used to transmit the information can be more or less energy efficient: for embedded systems, it becomes a critical aspect. The Internet-of-Things (IoT) has emerged as one of the leading research area for wireless communications as several billions connected devices are forecasted in years to come [1]. A significant part of communication transactions in the IoT are expected to be done through Low Power Wide-Area (LPWA) networks [2, 3], for which requirements include low cost and low energy consumption. A link budget improvement of 15/20dB in comparison to existing cellular technologies is expected [2], as reducing the costs to connect the devices to the wide-area network will encourage IoT deployment. To meet these requirements, the current generation of LPWA technologies dramatically extended the sensitivity performance of its receivers.

The sensitivity of a receiver is defined as the minimal power required to achieve an arbitrary level of error rate. It is commonly expressed as

$$\rho^{\mathrm{dBm}} = \mathrm{SNR}_{\mathrm{min}}^{\mathrm{dB}} + 10\log_{10}(BN_0), \tag{1}$$

*Corresponding author
Email addresses: yoann.roth@cea.fr (Yoann Roth), jean-baptiste.dore@cea.fr (Jean-Baptiste Doré), laurent.ros@gipsa-lab.grenoble-inp.fr (Laurent Ros), vincent.berg@cea.fr (Vincent Berg)

where B is the bandwidth of the signal (in Hz), $\mathrm{SNR}_{\min}$ the minimum Signal-to-Noise Ratio (SNR) to reach the level of error rate, and N_0 the spectral density of the noise in mW/Hz (with $10\log_{10}(N_0) \simeq -174$dBm/Hz at 20°C). In Equation (1), ρ is expressed in dBm, *i.e* 10 times the log of the ratio of the power expressed in mW. The energy efficiency of a physical layer can be estimated from the energy per bit to noise spectral density ratio, denoted by E_b/N_0. This metric shows how efficiently the energy is used: the lower is the required E_b/N_0, the more energy efficient is the technology. The relationship between the SNR and the energy efficiency is

$$\mathrm{SNR} = \frac{R}{B} \cdot \frac{E_b}{N_0} = \eta \cdot \frac{E_b}{N_0}. \tag{2}$$

where R is the data rate and $\eta = R/B$ is the spectral efficiency of the technology, expressed in bits/s/Hz. A different expression of the sensitivity, regardless of the bandwidth, can then be given as

$$\rho^{\mathrm{dBm}} = \left(\frac{E_b}{N_0}\right)^{\mathrm{dB}}_{\min} + 10\log_{10}(R) + 10\log_{10}(N_0). \tag{3}$$

This expression clearly explains the current trend of LPWA networks towards low data rate: if the value of R is reduced, lower levels of sensitivity are required to guarantee the quality of service and longer range of communication may be provided by the system.

Reducing the data rate can be done by reducing the bandwidth B for a constant spectral efficiency, or by reducing the spectral efficiency η for a constant bandwidth B. The first solution leads to narrow-band signaling, the option chosen by the IoT company Sigfox [4]. Dealing with narrow-band signals involves some technological issues, as it implies long durations of emitted signals. The second option, reducing the value of η, is often done by the use of the well-known spreading factor, or repetition factor. Indeed, repeating by a factor λ divides both the values of η and $\mathrm{SNR}_{\min}$ by the same factor, thus lowering the sensitivity level (when the bandwidth is fixed).

However, neither of these techniques change the energy efficiency, as the required E_b/N_0 is intrinsic to the modulation used. It is furthermore bounded by the Shannon's limit of the information theory [5], which defines the maximum transmission rate with arbitrarily low bit-error probability, for a given SNR and bandwidth. A formulation of this limit can be [6]

$$\frac{E_b}{N_0} \geq \frac{2^{\eta} - 1}{\eta}, \tag{4}$$

thus giving the minimum E_b/N_0 (*i.e* maximum energy efficiency) for a reliable communication as an increasing function of the spectral efficiency, with the ultimate limit $E_b/N_0 = -1.59$dB when η tends toward 0. As having a system's performance close to this ultimate limit would imply an optimal use of the energetic resource for a given spectral efficiency, it is clear that decreasing the required E_b/N_0 should be a major concern.

An interesting option to combine both E_b/N_0 and η reduction is the use of M-ary orthogonal modulations. Indeed, by increasing the size of the alphabet M, the spectral efficiency (given by $\log_2(M)/M$) is reduced and the energy efficiency is increased, eventually reaching the Shannon's limit for an infinite value of M [6]. However, since the spectral efficiency becomes close to 0, this solution is quite unrealistic. It is nonetheless purportedly used by a current commercial off-the-shelf long range solution, supported by the LoRa Alliance [7], as suggested by the patent [8] held by a company member of the alliance. Another option to reduce both E_b/N_0 and η is the use of channel coding [9]. In this area, the use of the turbo principle [10] has been shown to be particularly efficient, but implies high consumption at the receiver side. Even though the transmitter for this scheme has a low complexity, most of the current LPWA solutions rely on other Forward Error Correction (FEC) codes, and a potential improvement can be done by introducing more sophisticated receiver algorithms.

The use of orthogonal alphabet and coding in the same transmit process combined with a turbo receiver was first presented for the case of the binary Hadamard code in [11]. In [12], we proposed the Turbo-FSK scheme as an adaptation of [11], replacing the binary Hadamard codewords by the non-binary complex codewords of the orthogonal M-ary Frequency-Shift-Keying modulation (M-FSK). This modulation is an interesting choice as its constant envelope property provides a power efficient solution regarding the transmit power amplifier. The use of pure frequency waveforms also leads to robustness through frequency-selective multipath channel. Demodulation can be performed using the Fast-Fourier Transform (FFT), as in Orthogonal-Frequency-Division-Multiplexing (OFDM) receivers [13]. M-FSK is widely used for monitoring application, and off-the-shelf optimized chips are available [14]. Limitations of the Turbo-Hadamard code from [11] have been studied in [15], using the EXtrinsic Information Transfert (EXIT) Chart analysis [16] and its extension to multi-dimensional codes [17]. The EXIT analysis is used to observe the exchanges of information inside the decoder, and to predict the "waterfall" region of a turbo process, *i.e* the region where the Bit-Error Rate (BER) curve drops significantly.

In this paper, we propose to extend the initial analysis of the Turbo-FSK done in [12]. After presenting the modulation

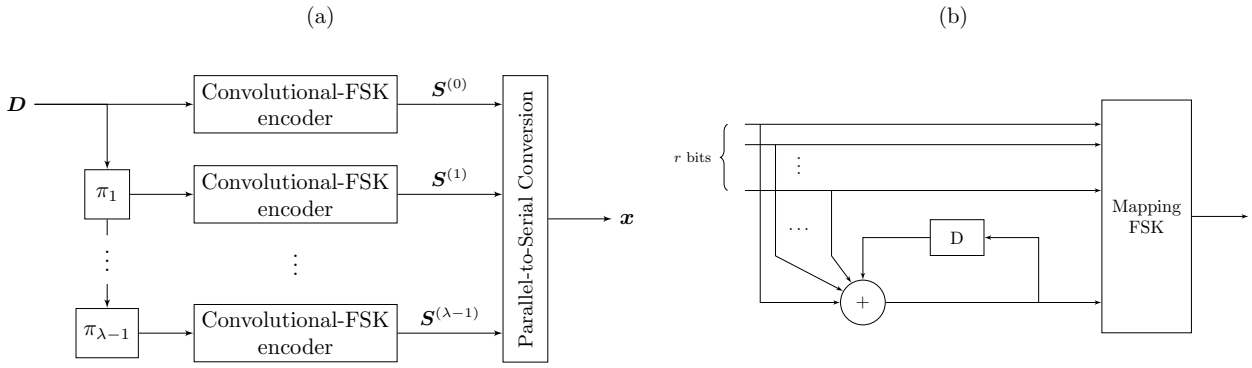

Figure 1: (a) The Turbo-FSK transmitter with λ stages. (b) The convolutional-FSK encoder

and demodulation procedures, we perform the EXIT analysis of the scheme, considering the modifications implied by the use of the FSK alphabet. Using this analytical tool, we optimize the parameters of the scheme by finding, for every set of parameters, the best pinch-off value. This value is defined as the E_b/N_0 value for which the decoder can recover without error the information word after a certain number of iterations. EXIT chart accurately predicts the convergence behavior of the iterative decoder for large interleaving depth. Considering the LPWA context, where short packet lengths are expected, we propose to perform extensive BER computation to confirm if the general trend obtained from the EXIT analysis is confirmed when the packet length is shortened. The scheme is then compared to state-of-the art modulations, including the Turbo Code standardized and used in the 3G and 4G standards [18]. This channel code is a natural candidate for the next generation of cellular IoT network, the Narrow-Band IoT (NB-IoT) recently released by the 3GPP [19].

The paper is organized as follows: the system model is introduced in Section 2, while the EXIT analysis and the parameters optimization are performed in Section 3. Performance of the scheme and comparison versus LPWA solutions are presented Section 4 and Section 5 concludes the paper.

2. System Model

For the following parts, bold lowercase letters denote row vectors, e.g. $\boldsymbol{x}$, and bold uppercase letters matrices, e.g. $\boldsymbol{X}$. The Discrete Fourier Transform (DFT) matrix of size $2^r \times 2^r$ is denoted $\boldsymbol{F}_r$. j is the unit imaginary number, $\overline{z}$ the complex conjugate of z and $\boldsymbol{Z}^{\mathrm{H}}$ is the Hermitian transpose of the matrix $\boldsymbol{Z}$. $\mathrm{Re}(z)$ (resp. $\mathrm{Im}(z)$) is the real part (resp. imaginary part) of complex number z.

2.1. Transmitter

We denote $\boldsymbol{D}$ the information bit matrix of size $P \times r$, which elements are $\{b_{p,n}\}$, with $p \in \{0, ..., P-1\}$ and $n \in \{0, \dots r-1\}$. We assume that the information bits are independent and equiprobable. The transmitter is shown in Figure 1 (a). It is composed of λ stages, each one having for input an interleaved version of $\boldsymbol{D}$.

The convolutional-FSK encoder is presented in Figure 1 (b). The encoding process consists in adding one redundancy bit, computed as the accumulated parity of the r input bits. The $r+1$ bits are then mapped to the FSK alphabet, which contains 2^{r+1} codewords. Because of this encoding, each of the P codewords is linked to the previous one. An extra codeword is appended to set back the memory to 0, leading to a total of $P+1$ FSK codewords of length M. The alphabet $\boldsymbol{A}$ can be constructed as orthogonal or bi-orthogonal. In the orthogonal case, $\boldsymbol{A} = \boldsymbol{F}_r$ and $r = \log_2(M) - 1$. In the bi-orthogonal case, $\boldsymbol{A} = [\boldsymbol{F}_r; -\boldsymbol{F}_r]$ and $r = \log_2(M)$. Each stage output $\boldsymbol{S}^{(k)}$, $k \in \{0, \dots \lambda-1\}$, is then a $(P+1) \times M$ matrix, and all the codewords are concatenated in a serial way to be sent through the transmission channel, giving the $(P+1)M\lambda$ elements of the vector $\boldsymbol{x}$. The code is entirely described by the parameters M, λ and N. The spectral efficiency of the scheme is defined as

$$\eta = \frac{N}{(N/r+1)M\lambda} \approx \frac{r}{M\lambda}, \tag{5}$$

where N is the information block size with $N = Pr$. The approximation is valid when a large value of N is considered.

For illustration purpose, a typical mapping of the FSK alphabet is represented on the Figure 2, along with the oversampled time representation and the spectrum of each codeword.

2.2. AWGN channel and its parameters

The discrete vector $\boldsymbol{x}$ is transformed into an analog signal by using chip pulse at chip-time $T_c = \eta/R = 1/B$. After up transposition to carrier frequency, the RF real signal is transmitted over an AWGN channel with monolateral bandwidth

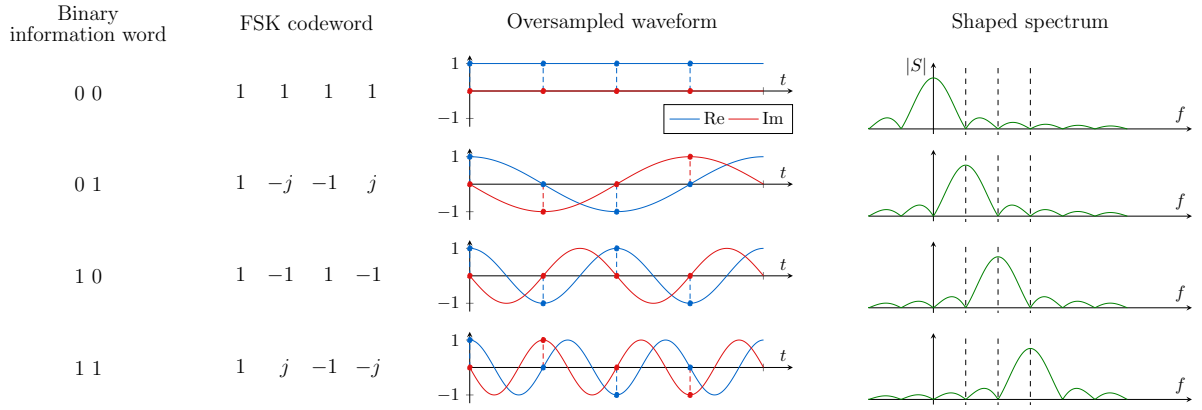

Figure 2: Example of the mapping of the FSK codewords for the case $M = 4$, and representation of the oversampled time waveform and the spectrum S after time-domain rectangular shaping.

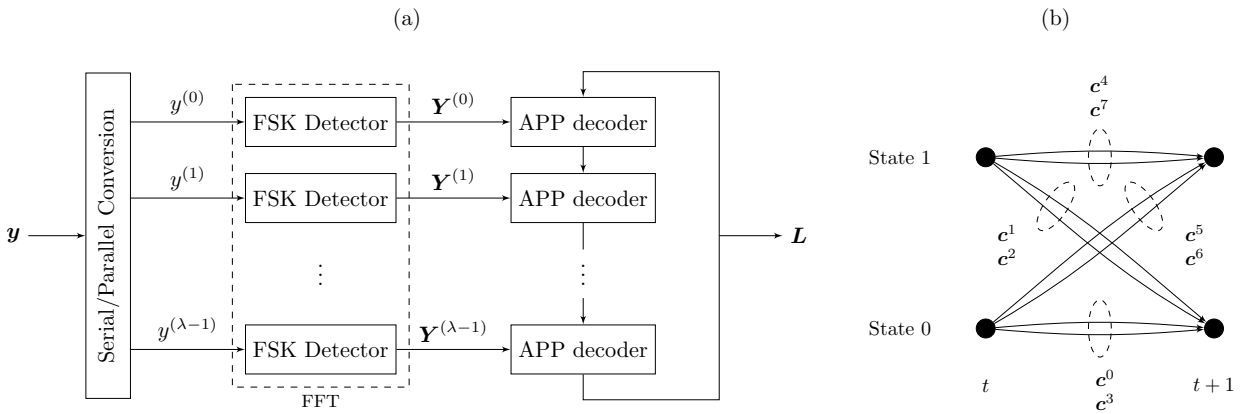

Figure 3: (a) The Turbo-FSK receiver with λ stages. (b) Trellis of the Turbo-FSK, for an orthogonal alphabet and $M = 8$

$B = 1/T_c$, noise monolateral spectral density N_0 and useful signal average power $P_x = E_b\eta/B$. At the receiver side, after frequency down conversion, chip matched filter, and sampling at every T_c, the discrete model of the baseband signal can be expressed in vector form as

$$\boldsymbol{y} = \boldsymbol{x} + \boldsymbol{n}, \tag{6}$$

where $\boldsymbol{n}$ is a zero-mean circular complex white noise. All vectors are composed of $(P+1)M\lambda$ chips. Each element of $\boldsymbol{n}$ are independant and have a variance equal to $\sigma^2 = N_0 B$, and the power of the signal $\boldsymbol{x}$ is equal to P_x.

2.3. Receiver

The Turbo-FSK receiver is depicted in Figure 3 (a). After a Serial-to-Parallel conversion, the λ vectors $\boldsymbol{y}^{(k)}$ (with $k \in \{0, \dots \lambda\}$) of $P+1$ orthogonal codewords are fed to the FSK detector. This block consists in performing the projection of each codewords in $\boldsymbol{y}^{(k)}$ over the alphabet of all possible codewords, *i.e* performing the matrix operation $\boldsymbol{y}^{(k)}\boldsymbol{A}^{\mathrm{H}}$. Since a FSK alphabet has been chosen, this step can be performed using the Fast-Fourier Transform (FFT) algorithm. The output $\boldsymbol{Y}^{(k)}$ is a $(P+1) \times 2^{r+1}$ matrix, which will be used as channel observations by its associated decoder. The turbo principle consists in exchanging iteratively information between the decoders. After the appropriate deinterleaving, a decoder will use both the channel observation and the extrinsic information from all the other decoders (the *a priori* information) to perform a new estimation of the information bits. The exchanged information between the decoders, denoted as $\boldsymbol{L}$ in Figure 3, is the Log Likelihood Ratio (LLR) of the information bits, defined as

$$\boldsymbol{L} = \left\{ L(b_{p,n}) = \log \frac{p(b_{p,n}=0)}{p(b_{p,n}=1)} \right\}_{\substack{p\in\{0,\dots,P-1\} \\ n\in\{0,\dots,r-1\}}}, \tag{7}$$

where $p(b_{p,n} = 1)$ (resp. $p(b_{p,n} = 0)$) is the probability that the bit $b_{p,n}$ equals 1 (resp. 0). The initial value for matrix $\boldsymbol{L}$ is all-zero, and does not include information about the trellis termination bits. While the sign of $L(b_{p,n})$ gives the hard value of the bit, its magnitude gives the reliability. At the end of every iteration, the matrix $\boldsymbol{L}$ includes the information from all the decoders, and a decision can be made on the information bits.

2.4. Probabilistic Decoding

Each decoder performs an estimation of the information bits by computing the *A Posteriori* Probabilities (APP) of the bits. We consider the received noisy FSK codeword $\boldsymbol{y}^p$, $p \in \{0, \dots P-1\}$ from the k-th stage. $\boldsymbol{d} = \{d_n\}_{n\in\{0,\dots r-1\}}$ is the decoded information word. $\boldsymbol{c}^i$ is a codeword from the FSK alphabet $\boldsymbol{A}$, and $\boldsymbol{b}^i = \{b_n^i\}_{n\in\{0,\dots r-1\}}$ its associated information word ($i \in \{0, \dots 2^{r+1}-1\}$). The APP of a codeword is the probability of having the codeword knowing the observation, and

$$p(\boldsymbol{c}^i|\boldsymbol{y}^p) = \frac{p(\boldsymbol{y}^p|\boldsymbol{c}^i)\ p(\boldsymbol{c}^i)}{p(\boldsymbol{y}^p)}, \tag{8}$$

by applying Bayes' theorem. $p(\boldsymbol{c}^i)$ is the *a priori* probability of having the codeword $\boldsymbol{c}^i$, or that the decoded information word $\boldsymbol{d}$ is $\boldsymbol{b}^i$. Introducing Y_i^p the i-th component of the DFT of $\boldsymbol{y}^p$, the APP becomes [12]

$$p(\boldsymbol{c^i}|\boldsymbol{y}^p) = C \exp\left\{\frac{1}{\sigma^2}\,\mathrm{Re}\,(Y_i^p) + \sum_{n=0}^{r-1}\frac{1-2b_n^i}{2}L(d_n)\right\}, \tag{9}$$

with C a constant eliminated in further computations.
This expression conveniently uses the DFT of the received codeword, *i.e* the channel observation, and a particular combination of the LLR $L(d_n)$. The use of a memory in the encoding process, as described Figure 1 (b), induces the construction of a trellis. The Bahl, Cocke, Jelinek and Raviv (BCJR) [20] algorithm can be used to decode the trellis, as suggested in [11]. Denoting $\boldsymbol{c}^i$, $i \in \{0, 2^{r+1}-1\}$ the codewords of the alphabet, the trellis for the special case of an orthogonal alphabet and $M = 8$ is depicted on the Figure 3 (b). Each state transition is encoded by 2^{r-1} codewords (*i.e* 2 is this case). Due to the orthogonality of the alphabet, every transition is orthogonal to each other. This orthogonality between the transitions is a fundamental characteristic of the code. For one particular section of the trellis, the BCJR algorithm will update the codewords probabilities with the knowledge of all the other sections. The updated probabilities are denoted $P(\boldsymbol{c^i}|\boldsymbol{y}^p)$.
The LLR of the information bits can be computed with [21]

$$L(d_n|\boldsymbol{y}^p) = \log \sum_{i\in\mathcal{B}_0^n} P(\boldsymbol{c}^i|\boldsymbol{y}^p) - \log \sum_{i\in\mathcal{B}_1^n} P(\boldsymbol{c}^i|\boldsymbol{y}^p), \tag{10}$$

where $\mathcal{B}_0^n$ (resp $\mathcal{B}_1^n$) are the codewords indexes associated to an information word for which bit n equals 0 (resp 1), with $n \in \{0, \dots r-1\}$.

Complexity of the Maximum *A-Posteriori* (MAP) algorithm presented here can be reduced using the max log approximation

$$\log\left(\sum_i e^{x_i}\right) \simeq \max_i(x_i). \tag{11}$$

This simplification will induce some performance loss, but reduces the computations to sum and max operations. Under AWGN consideration, it also allows the system to work without any Channel State Information (CSI), as the term σ^2 from (9) will be eliminated during the computations.

3. EXIT Chart Analysis

The Turbo-FSK scheme offers two adjustable parameters, M and λ. They can be optimized for better energy efficiency. However, a theoretical approach must be done to find the best set of parameters. A useful tool for iterative process analysis is the EXIT Chart, or the tracking of the exchanges of information between the decoders. It was first introduced by ten Brink [16], for the particular case of Parallel Concatenated Convolutional Codes (PCCC), or Turbo Codes (TC).

The idea of the EXIT Chart is to compute the extrinsic information from the output of the decoder for a certain amount of *a priori* information, which is simulated using a model. The metric used to measure the quantity of information is the Mutual Information (MI). Considering two sources of information X and Y and assuming that X is a binary source with equiprobable possible values $+1$ or -1, the MI between these two sources is

$$I(X,Y) = \frac{1}{2}\sum_{x=\pm1}\int_y f_{Y|X}(y \mid X=x).\log\frac{2f_{Y|X}(y \mid X=x)}{f(y|x=+1)+f(y|x=-1)}\mathrm{d}y, \tag{12}$$

with f the probability density functions. The value of the MI is between 0 (independence between the two sources) and 1 (complete correlation).

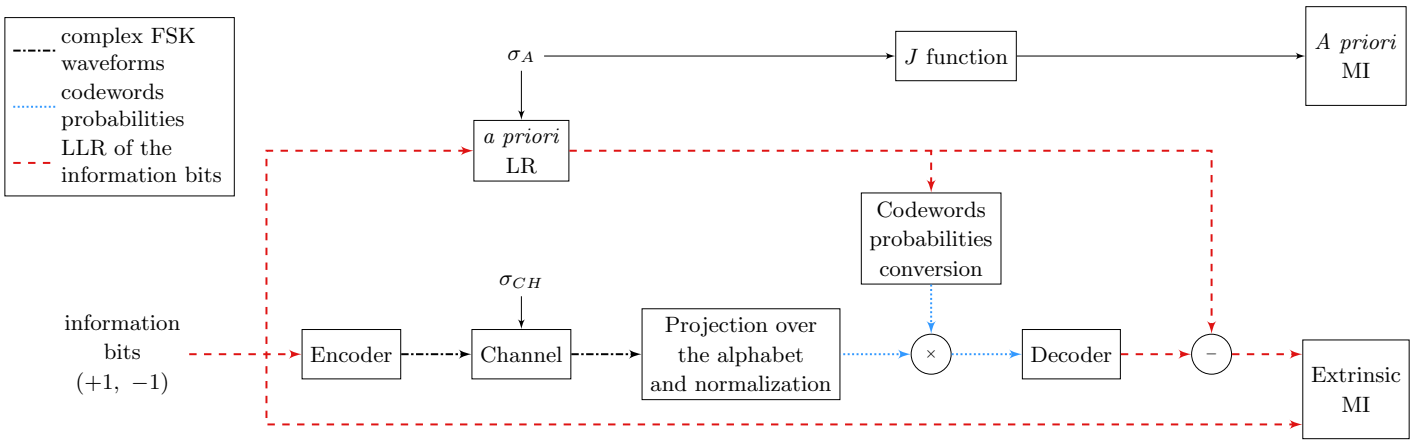

Figure 4: The EXIT Chart computation

3.1. A priori model

The *a priori* information model chosen is the standard Gaussian model $\mathcal{N}(\mu_A, \sigma_A)$, as suggested in [16]. The observation of the exchanged LR in the decoder allows us to validate this hypothesis. Assuming the consistency of the LR, we have $\mu_A = \sigma_A^2/2$, such that the model is now described by only one parameter. The *a priori* LR are expressed

$$L_A = \mu_A \cdot x + n_A \tag{13}$$

where x is the information ($x = \pm 1$) and n_A is a real white Gaussian noise with zero-mean, with standard deviation σ_A. The MI between the information source X and the *a priori* source can be expressed with the function J defined in [16], giving

$$I_A = J(\sigma_A) = 1 - \int_{-\infty}^{+\infty} \frac{1}{\sqrt{2\pi}\sigma_A} \exp\left\{-\frac{1}{2\sigma_A^2}\left(z - \frac{\sigma_A^2}{2}x\right)^2\right\} \log\left(1 + e^{-z}\right) dz. \tag{14}$$

3.2. Extrinsic information

The output of a decoder can be separated into three types of information: the *a priori* information L_A, the channel observation L_{ch} and the extrinsic information L_E generated by the decoder. The output LR is thus expressed

$$L = L_A + L_{\text{ch}} + L_E. \tag{15}$$

Extracting L_E can be realized by simply substracting the two other informations from the output LR L. The classic TC construction of a codeword includes a systematic part, *i.e* the uncoded information bits, and a parity part, or the redundancy bits added by the encoder. Obtaining the channel observation of the systematic bits and computing the extrinsic LR is then straightforward. However, in the Turbo-FSK case, the construction of the codewords does not include any systematic part: the codewords are elements of the DFT matrix, composed of complex symbols. The channel observation L_{ch} cannot be retrieved: decoding only the FSK modulation (without decoding the trellis) would still include the extrinsic information of the orthogonal code itself. This residual information from the channel must be taken into account for further interpretations.

3.3. Multi-dimensional EXIT Chart

When two decoders are used, the exchange of information between the decoders during the successive iterations can be represented in a two dimension plot. The case where the iterative process includes more than two decoders has been studied in [17]. If λ decoders are considered, the representation of the exchanges needs to be done in λ dimensions. Graphical interpretation becomes impossible for $\lambda > 3$, but for the special case where all decoders are the same (which is the case for the Turbo-FSK), a two-dimensional projection may be computed. If this projection does not intersect with the line going from $(0, 0)$ to $(1, 1)$, it indicates that convergence toward the maximum of MI is possible. The formula of the *a priori* MI must be changed [17] to

$$I_A = J\left(\sqrt{\lambda - 1} \cdot \sigma_A\right). \tag{16}$$

This formula can be interpreted as the fact that each decoder receives information from the $\lambda - 1$ other decoders.

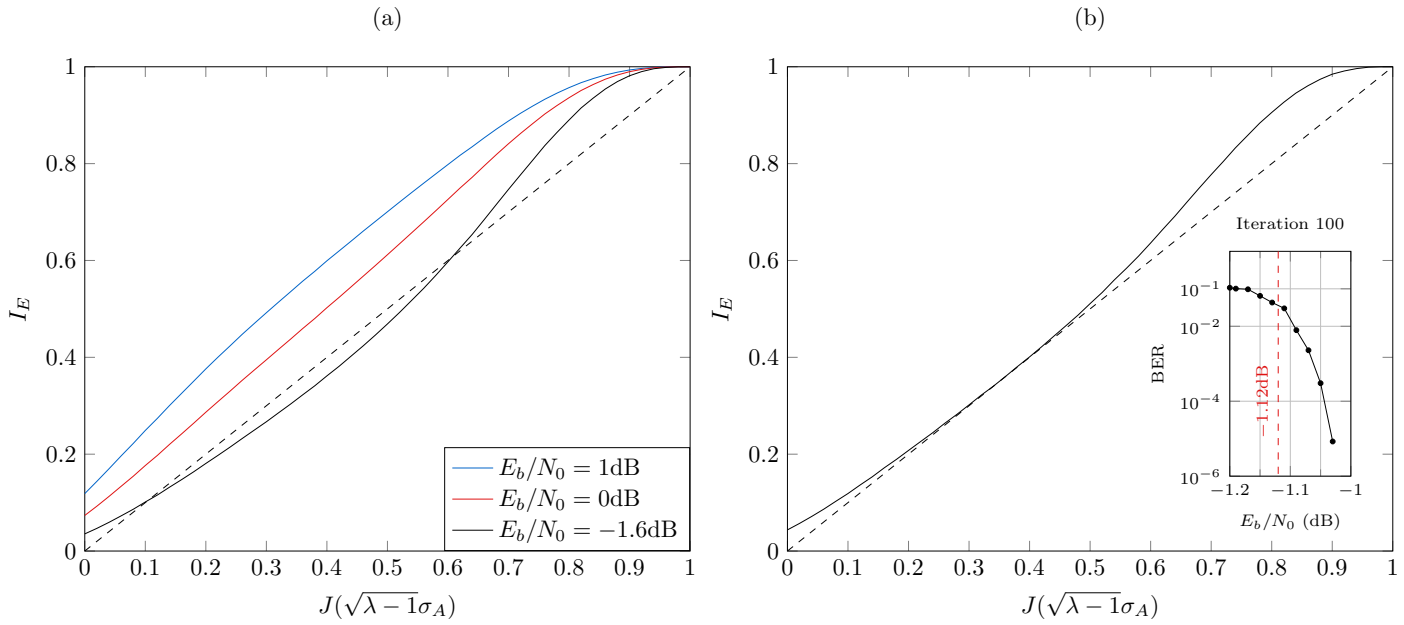

Figure 5: (a) EXIT Charts of the Turbo-FSK decoder with parameters $M = 128$, $\lambda = 4$, for various values of E_b/N_0. The information block size was set to $N = 100000$. (b) EXIT Chart and BER performance of the Turbo-FSK scheme with parameters $M = 128$, $\lambda = 4$. The EXIT Chart is computed for $E_b/N_0 = -1.12$dB and the information block size was set to $N = 100000$. BER performance is computed using $N = 100000$ and the MAP algorithm.

3.4. EXIT Chart Computation

The process to compute the EXIT Chart is depicted Figure 4. As previously mentioned, the code is not systematic, implying the impossibility to extract the channel observation and the necessity to convert the *a priori* LR to codewords probabilities. The subtraction after the decoder will give an extrinsic information that still contains the channel observation. The extrinsic MI block computes the integrals summation from (12). The *a priori* MI is computed using function J from (14) and the correction of (16). For a specific value of σ_{ch}, the extrinsic MI is computed for several values of σ_A, so that the *a priori* MI spans between 0 and 1. The EXIT Chart computation does not depend on the interleaving function, and needs to be done using very large block sizes, to ensure a good statistic for the density probability functions estimations (this assumption also implies statistical independence of all incoming messages into the decoder).

The EXIT Chart computations result for three values of E_b/N_0 are depicted on Figure 5 (a), along with the middle line $(0, 0) \rightarrow (1, 1)$. Turbo-FSK scheme with parameters $M = 128$, $\lambda = 4$ is selected, using an orthogonal alphabet, an information block size of $N = 100000$ is chosen and the MAP algorithm. For $E_b/N_0 = -1.6$dB, the EXIT Chart intersects the middle line around $I_A \simeq 0.1$. It can be concluded that whatever is the number of iterations, the decoding process cannot converge towards the error-free information word for this E_b/N_0 value. However, for E_b/N_0 values of 0 and 1dB, there is no intersection with the middle line: the process will then, after a certain number of iterations, successfully retrieve the exact information word.

An exhaustive search using these parameters shows that the smallest value of E_b/N_0 for which the EXIT Chart does not intersect with the middle line, or the "pinch-off" value, is $E_b/N_0 = -1.12$dB. The EXIT Chart for this value is illustrated Figure 5 (b), along with the BER performance of the Turbo-FSK scheme with the same parameters, and 100 decoding iterations. The EXIT Chart predicts accurately the beginning of the "waterfall" region, *i.e* the E_b/N_0 region where the BER drops significantly. Indeed, after the pinch-off value, the BER decreases to reach a value of 10^{-5} at $E_b/N_0 = -1.03$dB.

3.5. Parameters optimization

A way to optimize the energy efficiency of the scheme is to reduce the E_b/N_0 needed to reach an arbitrary level of error rate; for a given error rate (and a fixed binary information rate), the transmitted power is also reduced when the E_b/N_0 is decreased. The performance of the Turbo-FSK scheme directly depends on the value of parameters M, λ and N, the information block size. Since the EXIT Chart predicts the waterfall region, minimizing the pinch-off value will give the most efficient scheme under the assumed hypothesis. An exhaustive search of the pinch-off value is done for every set of parameters (M, λ), using an orthogonal alphabet. Coherent detection of the FSK is assumed and MAP algorithm without any approximation is used. The results are presented in Table 1. For each value M, we denoted with a * symbol the lowest pinch-off value depending on λ, and the overall lowest pinch-off is in bold. Results shows that Shannon ultimate capacity

λ \ M	16	32	64	128	256	512	1024	2048
2	2.23	1.61	1.15	0.86	0.53	0.30	−0.13	−0.61
3	0.33	−0.17	−0.59	−0.94	−1.23*	**−1.30***	−1.19*	−1.07*
4	0.02	−0.46	−0.84	−1.12*	−1.20	−1.04	−0.83	−0.59
5	−0.06*	−0.51*	−0.86*	−1.09	−1.03	−0.77	−0.47	−0.18
6	−0.06*	−0.51*	−0.84	−1.02	−0.84	−0.52	−0.14	0.19

Table 1: Pinchoff values in E_b/N_0 for every M and λ tested. EXIT Chart are computed using an information block size $N = 100000$. Best value for each M is denoted with a symbol *, and best couple of parameters is in bold.

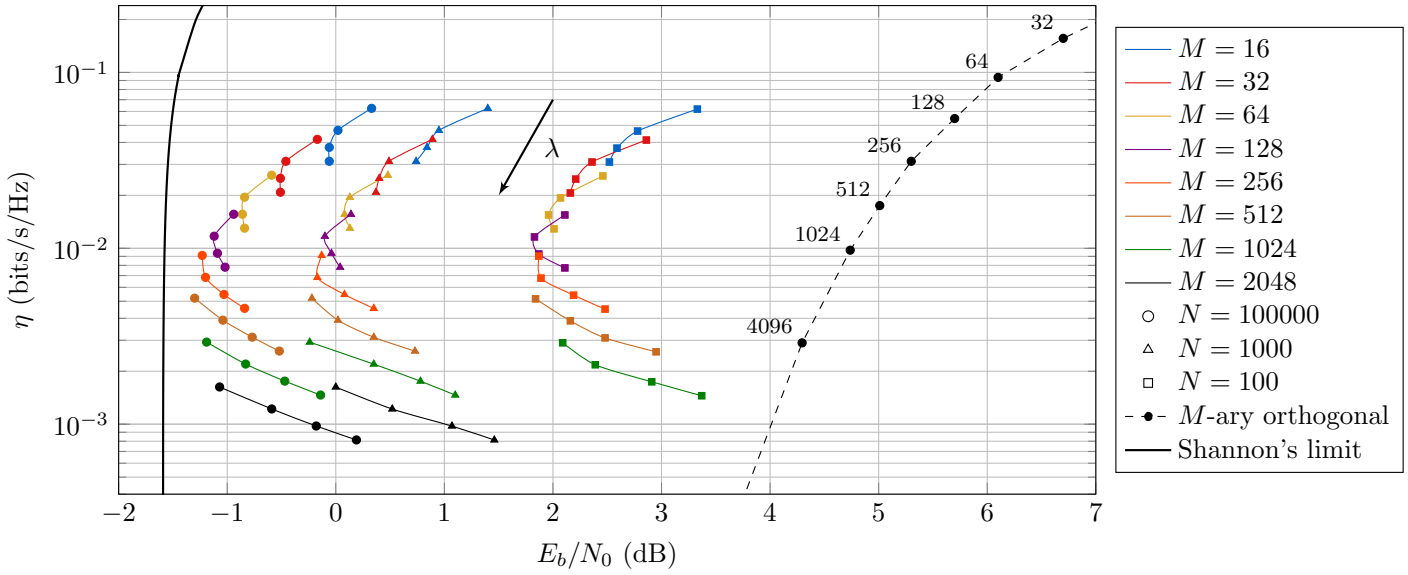

Figure 6: Values from Table 1 (EXIT Chart analysis with $N = 100000$) and BER simulation for $N = 1000$ and $N = 100$ in the plot normalized spectral efficiency versus energy efficiency.

($E_b/N_0 \simeq -1.56$dB for this spectral efficiencies) can be approached by only 0.29dB, using the set of parameters $(512, 3)$. A similar result was shown in [15], where a Hadamard systematic bi-orthogonal alphabet was used. The performance depending on the value of λ is not predictable, justifying the exhaustive approach for the optimization.

These results show the good asymptotic performance of the code. However, for the considered LPWA scenario, the size of the payload should be limited to a few bytes, up to a few hundreds of bytes. Small information block sizes are expected, but the EXIT Chart analysis is inaccurate when the value of N is small [16]. We can nonetheless perform BER computations to evaluate the performance depending on the set of parameters. For each set, we choose $N = 1000$ and $N = 100$ bits and search the E_b/N_0 value for which the BER reaches 10^{-4}. 10 decoder iterations and a random interleaver are used for the simulations. To depict the results, the normalized spectral efficiency of the scheme using the different sets of parameters, as defined in (5) is proposed. Results can be compared to the ultimate Shannon limit as defined by (4), and are depicted Figure 6. For each alphabet size, λ value from 3 to 6 are represented. Since increasing λ lowers the normalized spectral efficiency, the point with the highest η is $\lambda = 3$, then 4, and so on. The figure clearly shows the optimum value for the parameters, for both EXIT and BER analysis. The general trend obtained with the EXIT Chart seems to be confirmed even when the block size is shortened. Reducing the block size to $N = 1000$ bits (125 bytes) induces a performance loss of approximately 1dB (on average), implying a minimum gap to Shannon's limit equals to 1.35dB. For a block size of $N = 100$, the performance loss compared to the asymptotic pinch-off is 3dB, with the best set of parameters $(128, 4)$ being 3.42dB away from Shannon's limit.

4. Performance

As the Turbo-FSK parameters have been optimized to allow high energy efficiency, our interest goes into comparing the performance of the scheme against current published LPWA solutions. Comparisons are done versus three other state-of-the-art Machine-to-Machine (M2M) transmission schemes: the IEEE 802.15.4k standard [22], the LoRa physical layer, as described in the patent [8], and the serial concatenation of a TC [18, 23] with a M-FSK modulation.

4.1. Proposed solutions

For each solution, the physical layer is first described. Since mostly the transmitter side is discussed in the literature, we assume for each scheme the receiver to be the dual receiver version of the transmitter, with soft decoding (MAP) and demodulation when possible. The parameter λ is introduced, which will allow the spectral efficiency to be modulated for comparison purpose.

4.1.1. IEEE 802.15.4k

The IEEE 802.15.4k is a standard designed for local and metropolitan area networks. It is part of the Low-Rate Wireless Personal Area Networks (LR-WPANs). This standard supports three PHY modes: DSSS with BPSK or Offset-Quadrature Phase Shift Keying (O-QPSK), or 2-FSK. Since DSSS with BPSK modulation is the more robust scheme, we select this configuration. The standard specifications allow the use of a spreading factor value λ from 16 to 32768. In addition to the modulation and the spreading factor, the standard uses a Forward-Error-Correction (FEC). It is defined to be the convolutional code of rate 1/2, with generators polynomial [171 133] (in octal) and constraint length $k = 7$. An interleaving operation is considered between the steps of channel coding and modulation. The spectral efficiency of the scheme is defined as

$$\eta_1 = \frac{1}{2\lambda}. \tag{17}$$

Soft decoding using the well-known soft-input soft-output Viterbi decoder is considered.

4.1.2. OSSS with block code

Non-linear modulations based on an alphabet of M-ary orthogonal waveforms are known to be energy efficient, and to reach channel capacity for infinite size of alphabet [6], as discussed in the introduction of this paper. This property can be extended to Orthogonal Sequence Spread Spectrum (OSSS), and is purportedly used by the LoRa technology [8] with a Hamming block code in addition. For this study, we consider a Hamming block code of rate 4/7. The parity bits can be punctured to increase the rate. We denote by p the number of parity bits ($p \in \{0, 1, \dots 3\}$). After the encoding, the transmitter consists in an interleaver and an orthogonal modulation of size 2^λ. The spectral efficiency is equal to

$$\eta_2 = \frac{4}{4+p}\frac{\lambda}{2^\lambda}. \tag{18}$$

The receiver side consists in a soft demodulation, and soft Hamming decoding.

4.1.3. The UMTS/LTE TC

The recent 4G standard specification includes a TC [18]. Turbo codes are known to be very effective FEC schemes, and its use in the Cellular-IoT context is considered. They consist in the parallel concatenation of two identical recursive systematic convolutional codes. In the specification, each code is rate 1/2, of constraint length $k = 4$ with feedback and generator polynomials [13 15] (in octal). The overall rate of the TC is approximately 1/3 (extra few bits are required to close the trellis). With this FEC, we consider an orthogonal modulation of size M, and a spreading factor λ. The spectral efficiency can be expressed

$$\eta_3 = \frac{\log_2(M)}{3\lambda M}. \tag{19}$$

The receiver side consists in a turbo receiver [10, 23]. The use of soft iterative decoding implies high consumption at the receiver side, but complexity at the transmitter side is rather low. This scheme, denoted as FSK + TC in the sequel, is an interesting element of comparison against our proposed Turbo-FSK scheme. Indeed, it also implies the use of a powerful channel code and an orthogonal modulation, but in two successive steps, instead of the joint process used in the Turbo-FSK scheme.

4.2. Performance comparison

To compare the different schemes, we compute simulations for the AWGN channel, with coherent reception and ideal synchronization. Random interleavers are used, except for the TC UMTS where the interleaver specified by the 3G standard is used. The packet size is set to $N = 1000$. For the iterative receivers, 10 iterations are performed (TC and Turbo-FSK), and the MAP algorithm without any approximation is used. We choose, for the Turbo-FSK, the parameters $M = 128$ and $\lambda = 4$, *i.e* the best couple of parameters for this size of alphabet. The spectral efficiency is equal to $\eta = 1.17 \cdot 10^{-2}$ for these parameters. For each scheme, we can choose a different value of λ in order to equalize the spectral efficiency of the schemes. The selected parameters are summarized in Table 2.

Figure 7 (a) depicts the BER performance versus E_b/N_0 for the selected parameters. The scheme OSSS uses the Hamming code, which is less powerful than the convolutional code of the IEEE 802.15.4k standard, but offers better

PHY-layer	802.15.4k	OSSS	FSK+TC	Turbo-FSK
Modulation	DBPSK	512-Orthog	128-FSK	128-FSK
FEC	CC [171 133]	Hamming	TC [13 15]	Turbo-FSK
Binary code-rate	1/2	4/6	1/3	-
λ	43	9	2	4
η $(\cdot 10^{-2})$	1.163	1.172	0.907	1.170

Table 2: Parameters used for comparison.

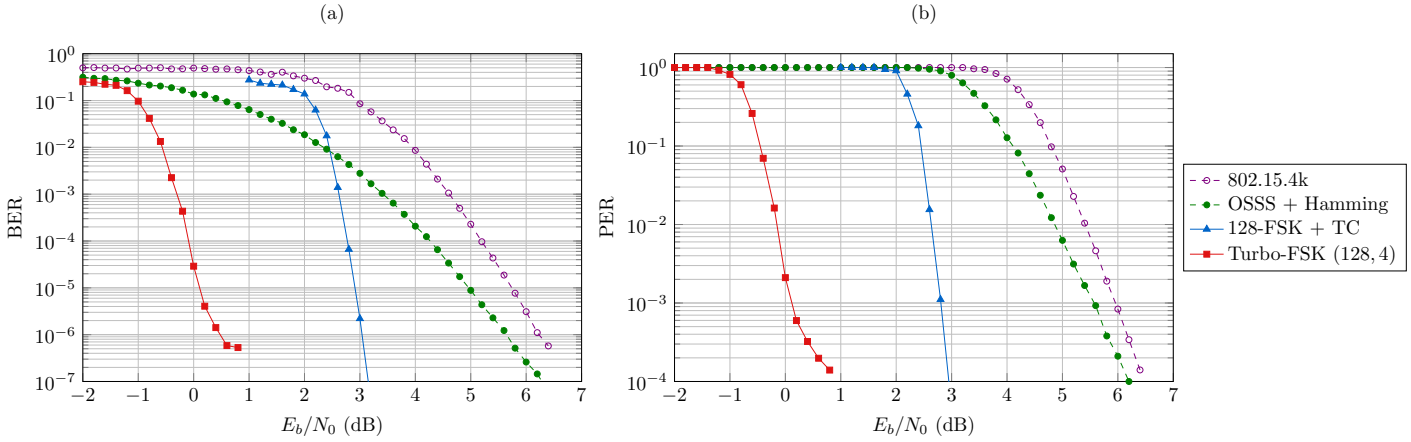

Figure 7: (a) BER and (b) PER performance comparison versus E_b/N_0, using the parameters given Table 2. The packet size is set to 1000 bits.

performance when combined with a relatively large size of orthogonal alphabet (512). The gain using the turbo principle is illustrated by the performance of both the FSK + TC and the Turbo-FSK. The scheme FSK + TC reaches a BER of 10^{-5} for a E_b/N_0 value of 2.91dB, and the Turbo-FSK outperforms all the other scheme, showing a 4.8dB gain versus the OSSS + Hamming scheme for the same BER. The gain offered by the Turbo-FSK scheme versus the scheme FSK + TC also shows the benefit of jointly optimizing the modulation and the channel coding instead of treating them separately.

The Packet Error Rate (PER) versus E_b/N_0 is depicted on the Figure 7 (b). For a PER of 10^{-3}, the Turbo-FSK with these parameters outperforms the scheme OSSS + Hamming code by 5.5dB. This level of PER is reached for $E_b/N_0 = 0.12$dB. Using Equation (2), with the spectral efficiency given in Table 2, the equivalent SNR is equal to -19.2dB, demonstrating the ability of the system to work at low levels of SNR.

These two figures show the real benefit of turbo processing on the sensitivity gain. Because all the spectral efficiency are normalized, the E_b/N_0 gain can be interpreted as the sensitivity gain between two schemes, when the same data rate is considered (see Equation (3)). The 5.5dB gain between Turbo-FSK versus the LoRa based scheme for a PER or 10^{-3} means that the sensitivity will be lower using our scheme. This can be interpreted as a potential reduction of the transmit power by a factor 3.5 while ensuring the same level of performance, or a distance increase by a factor 1.8 (under the approximation of free path loss exponent equal to 2). Comparison with other scheme could be considered; the use of a turbo code with a linear modulation also offers a good tradeoff between performance and spectral efficiency.

The sensitivity performance improvements are done at the expense of an increase of complexity at the receiver side. As we focus on the complexity at the node level, having a more complex receiver at the base-station is acceptable. However, a recent study showed that the Turbo-FSK physical layer can be implemented on off-the-shelf components [24], demonstrating that the complexity increase can be handled by components with low computation capacity.

5. Conclusion

While global LPWA solutions aims at lowering the sensitivity, improving the energy efficiency should remain a major concern. The Turbo-FSK scheme proves to be a serious candidate for the PHY layer of LPWA networks, offering high energy efficiency with reasonable spectral efficiency. The optimization realized using the EXIT analysis and the performance versus State-of-the-Art solutions show that very interesting gain in sensitivity can be achieved. The best set of parameters is shown to be only 1.35dB away for Shannon's limit for a packet size of 128 bytes, a fair size in the M2M context. The Turbo-FSK demonstrates the positive impact of mixing orthogonal modulations and turbo processing, and achieves promising performance while ensuring low complexity and a constant envelope at the transmitter. Further studies

should however be considered about the complexity increase, and the synchronization, which can reveal itself arduous for the considered levels of SNR.

References

[1] Verizon, State of the Market: Internet of Things 2016 (April 2016).
URL http://www.verizonenterprise.com/verizon-insights/state-of-market-internet-of-things/2016/

[2] LTE-M - Optimizing LTE for the Internet of Things, Nokia White Papers.

[3] T. Rebbeck, M. Mackenzie, N. Afonso, Low-powered wireless solutions have the potential to increase the M2M market by over 3 billion connections, Analysys Mason.

[4] SigFox website, http://www.sigfox.com/, accessed: November 2, 2016.

[5] C. Shannon, A mathematical theory of communication, The Bell System Technical Journal 27 (3) (1948) 379–423. doi:10.1002/j.1538-7305.1948.tb01338.x.

[6] J. Proakis, Digital Communications 3rd Edition, Communications and signal processing, McGraw-Hill, 1995.

[7] LoRa Alliance, https://www.lora-alliance.org/, accessed: November 2, 2016.

[8] O. Seller, N. Sornin, Low power long range transmitter, US Patent 20140219329 A1.

[9] J. Costello, D.J., J. Forney, G.D., Channel coding: The road to channel capacity, Proceedings of the IEEE 95 (6) (2007) 1150–1177. doi:10.1109/JPROC.2007.895188.

[10] C. Berrou, A. Glavieux, P. Thitimajshima, Near Shannon limit error-correcting coding and decoding: Turbo-codes. 1, in: IEEE International Conference on Communications (ICC). Geneva., Vol. 2, 1993, pp. 1064–1070. doi:10.1109/ICC.1993.397441.

[11] L. Ping, W. Leung, K. Y. Wu, Low-rate turbo-Hadamard codes, IEEE Transactions on Information Theory 49 (12) (2003) 3213–3224. doi:10.1109/TIT.2003.820018.

[12] Y. Roth, J.-B. Dore, L. Ros, V. Berg, Turbo-FSK: A New Uplink Scheme for Low Power Wide Area Networks, in: 2015 IEEE 16th International Workshop on Signal Processing Advances in Wireless Communications (SPAWC), 2015, pp. 81–85. doi:10.1109/SPAWC.2015.7227004.

[13] K. Kikuchi, M. Osaki, Highly-sensitive coherent optical detection of M-ary frequency-shift keying signal, Optics Express 19 (26) (2011) B32–B39.

[14] SX1272 from Semtech, datasheet, http://www.semtech.com/wireless-rf/rf-transceivers/sx1272/, accessed: November 2, 2016.

[15] Y.-J. Wu, L. Ping, On the limiting performance of turbo-Hadamard codes, Communications Letters, IEEE 8 (7) (2004) 449–451. doi:10.1109/LCOMM.2004.832757.

[16] S. ten Brink, Convergence behavior of iteratively decoded parallel concatenated codes, IEEE Transactions on Communications 49 (10) (2001) 1727–1737. doi:10.1109/26.957394.

[17] S. ten Brink, Convergence of multidimensional iterative decoding schemes, in: Conference Record of the Thirty-Fifth Asilomar Conference on Signals, Systems and Computers, Vol. 1, 2001, pp. 270–274 vol.1. doi:10.1109/ACSSC.2001.986918.

[18] LTE Evolved Universal Terrestrial Radio Access (E-UTRA): Multiplexing and Channel Coding, 3GPP TS 36.212, V12.6.0, Release 12 (2015) 12–15.

[19] "Introduction of Rel-13 feature of NB-IoT in 36.212", 3GPP TSG RAN WG1 Meeting #85 R1-166045, Nanjing, China.

[20] L. Bahl, J. Cocke, F. Jelinek, J. Raviv, Optimal decoding of linear codes for minimizing symbol error rate (corresp.), IEEE Transactions on Information Theory 20 (2) (1974) 284–287. doi:10.1109/TIT.1974.1055186.

[21] J. Hagenauer, E. Offer, L. Papke, Iterative decoding of binary block and convolutional codes, IEEE Transactions on Information Theory 42 (2) (1996) 429–445. doi:10.1109/18.485714.

[22] 802.15.4k: Low-Rate Wireless Personal Area Networks (LR-WPANs) Amendment 5: Physical Layer Specifications for Low Energy, Critical Infrastructure Monitoring Networks., IEEE Standard for Local and metropolitan area networks (2013) 1–149.

[23] M. C. Valenti, J. Sun, The UMTS Turbo Code and an Efficient Decoder Implementation Suitable for Software-Defined Radios, International Journal of Wireless Information Networks 8 (4) (2001) 203–215. doi:10.1023/A:1017925603986.

[24] J. Estavoyer, Y. Roth, J.-B. Doré, V. Berg, Implementation and Analysis of a Turbo-FSK transceiver for a new Low Power Wide Area Physical Layer, in: 2016 International Symposium on Wireless Communication Systems (ISWCS): Special sessions (ISWCS'2016 - Special sessions), Poznan, Poland, 2016.